Journal of Peptide Science
J. Pept. Sci. 2008; **14**: 503–509
Published online 12 November 2007 in Wiley InterScience (www.interscience.wiley.com). DOI: 10.1002/psc.938

JOURNAL OF PEPTIDE SCIENCE

Combination of ellipsometry, laser scanning microscopy and *Z*-scan fluorescence correlation spectroscopy elucidating interaction of cryptdin-4 with supported phospholipid bilayers‡

ADAM MISZTA,[a] RADEK MACHÁŇ,[a] ALEŠ BENDA,[a] ANDRE J. OUELLETTE,[c] WIM TH. HERMENS[b] and MARTIN HOF[a]*

[a] J. Heyrovský Institute of Physical Chemistry v.v.i., Academy of Sciences of the Czech Republic, Czech Republic
[b] Cardiovascular Research Institute Maastricht and DELBIA bv, Maastricht University, Netherlands
[c] Departments of Pathology & Laboratory Medicine and Microbiology & Molecular Genetics, School of Medicine, University of California, Irvine, USA

Received 4 June 2007; *Revised 6 August 2007*; *Accepted 14 August 2007*

Abstract: The present study has two main objectives. The first is to characterize antimicrobial peptide (AMP) cryptdin-4 (Crp-4) interactions with biological membranes and to compare those interactions with those of magainin 2. The second is to combine the complementary experimental approaches of laser scanning microscopy (LSM), ellipsometry, and *Z*-scan fluorescence correlation spectroscopy (FCS) to acquire comprehensive information on mechanisms of AMP interactions with supported phospholipid bilayers (SPBs) – a popular model of biological membranes. LSM shows appearance of inhomogeneities in spatial distribution of lipids in the bilayer after treatment with Crp-4. Ellipsometric measurements show that binding of Crp-4 does not significantly change the lipid structure of the bilayer (increase in adsorbed mass without a change in thickness of adsorbed layer). Furthermore, Crp-4 slows the lateral diffusion of lipids within the membrane as shown by *Z*-scan FCS. All changes of the bilayer induced by Crp-4 can be partially reversed by flushing the sample with excess of buffer. Bilayer interactions of magainin 2 are significantly different, causing large loss of lipids and extensive damage to the bilayer. It seems likely that differences in peptide mode of action, readily distinguished using these combined experimental methods, are related to the distinctive β-sheet and α-helical structures of the respective peptides.

Keywords: cryptdin-4; magainin 2; supported phospholipid bilayers; ellipsometry; laser scanning microscopy; fluorescence correlation spectroscopy

INTRODUCTION

Antimicrobial peptides (AMPs) form a very large, diverse, and evolutionarily ancient collection of peptides with important roles in innate immunity in all multicellular organisms [1]. Although differing significantly in size and primary structure, most AMPs share common features: They are cationic under physiological conditions with a minimum electropositive charge of +2, and they are amphiphilic due to the spatial segregation of hydrophobic and cationic amino acid residues [1,2]. AMPs are extensively investigated for possible pharmacological applications, as antibiotics against which microbes develop little resistance [1], and as potential antitumor agents [3,4]. It is well established that AMP interactions with target cell membrane and its membrane permeation are key factors in their antibiotic activity. Therefore, analyses of interaction of AMPs with varied model membrane systems, including supported phospholipid bilayers (SPBs), using a variety of experimental techniques have led to the development of several models of AMP activity [2,5–7]. Still, many questions concerning the molecular details of interactions of individual AMPs with phospholipid bilayers remain to be answered.

In the present study, we combine ellipsometry with microscopic techniques to characterize changes of SPBs induced by the AMP cryptdin-4 (Crp-4). Crp-4 is the most bactericidal of the α-defensins produced by mouse Paneth cells [8–10] and has a relatively rigid secondary structure of three β-strands typical of defensins [1,8]. We also performed similar experiments for magainin 2, the well-characterized AMP isolated originally from the skin of the African frog *Xenopus laevis* [11]. Magainin 2 is a prototypical linear AMP that adopts α-helical conformation in contact with membranes [2,12,13]. Both peptides possess selective antibacterial activity due to preferential interactions with electronegative rather than zwitterionic phospholipid bilayers [1,9,13,14].

It seems likely that differences in peptide mode of action, readily distinguished using these combined experimental methods, are related to the distinctive β-sheet and α-helical structures of the respective peptides. Linear peptides adopt α-helices in hydrophobic

* Correspondence to: Martin Hof, J. Heyrovský Institute of Physical Chemistry v.v.i., Academy of Sciences of the Czech Republic, Dolejškova 3, 18223 Prague 8, Czech Republic; e-mail: hof@jh-inst.cas.cz
‡ This article is part of the Special Issue of the Journal of Peptide Science entitled "2nd workshop on biophysics of membrane-active peptides".

environments and accumulate within the bilayers until the integrity of the bilayer is disrupted. A vast majority of these α-helical AMPs seems to share a common mode of action [6], models of which (toroidal pore, carpet model etc.) are discussed elsewhere [2,5–7]. Some studies suggest that magainin 2 acts via pore formation (for example [15]), while according to others it acts via carpet model [6,12]. Previous works [9,10,16,17] have shown that Crp-4 is monomeric in solution and its bactericidal activity corresponds directly to the ability to bind to and permeabilize model membranes by a transient, graded leakage mechanism. It has been also shown that Crp-4 molecules do not insert as deep into the membrane as molecules of α-helical peptides do [13].

MATERIALS AND METHODS

Materials and Sample Preparation

SPBs were prepared from the following phospholipids: dioleoyl-phosphatidylcholine (DOPC) and dioleoyl-phosphatidylserine (DOPS) obtained from Avanti Polar Lipids (Alabaster, AL). Head group labeled phospholipid 1,2-dihexadecanoyl-sn-glycero-3-phosphoethanolamine (Oregon Green 488 DHPE, Invitrogen) was added for fluorescence measurements. A buffer with pH 7.4 containing 10 mM Hepes with 150 mM NaCl was prepared with pure water (Milli-Q3 system, Millipore, Etten-Leur, The Netherlands); 2 mM $CaCl_2$ was added for bilayer preparation.

Recombinant Crp-4 (GLLCYCRKGHCKRGERVRGTCGIRFLYCCPRR) (MW = 3756) was expressed in *Escherichia coli* as an *N*-terminal 6X-histidine tagged fusion protein in the pET28a expression vector (Novagen, Inc. Madison, WI) as described [9,18]. The Crp-4 molecule was purified to homogeneity using sequential nickel-nitrilotriacetic acid (Ni-NTA, Qiagen) resin affinity chromatography, and C18 reverse-phase high performance liquid chromatography (RP-HPLC). Peptide homogeneity was confirmed by acid-urea polyacrylamide gel electrophoresis (AU-PAGE) and by analytical C18 RP-HPLC [19–21]. Molecular masses of purified peptides were determined using matrix-assisted laser desorption ionization mode mass spectrometry (Voyager-DE MALDI-TOF, PE-Biosystems, Foster City, CA) in the UCI Biomedical Protein and Mass Spectrometry Resource Facility. Magainin 2 (GIGKFLHSAKKFGKAFVGEIMNS) (MW = 2466.90) was obtained from Sigma-Aldrich.

Freshly cleaved mica stacks of 5 mm diameter obtained from Metafix (Montdidier, France) were used as solid support for microscopic samples, and silicon wafers from Wacker Chemitronic (n-type, phosphorus doped) were used for ellipsometry. Small unilamellar vesicles (SUVs) were prepared by sonication according to Benes *et al.* [22] from a mixture of DOPC and DOPS in the molar ratio 4 : 1. Ratio of labeled to unlabeled phospholipid was 1 : 10 000 for laser scanning microscopy (LSM) and 1 : 100 000 for fluorescence correlation spectroscopy FCS. SPBs were formed by exposing a solid surface to a suspension of SUVs in a calcium containing buffer (Benes *et al.* [22]). Concentration of peptide used in all experiments was 1 μM. Initially, Crp4 was subjected to amino acid analysis, and then subsequent preparations were quantitated by absorption at 280-nm wavelength. The solution of magainin 2 was prepared by diluting a stock solution of known concentration obtained from Sigma Aldrich.

Confocal Fluorescence Microscopy

Two types of measurements – intensity scans and *Z*-scan FCS – were carried out on a MicroTime 200 inverted epifluorescence confocal microscope (Picoquant, Germany). We used a configuration containing a pulsed diode laser (LDH-P-C-470, 470 nm, Picoquant, Germany) providing 80 ps pulses at a 40 MHz repetition rate, a proper filter set (clean up filter HQ470/20, dichroic mirror 490DRLP, and band-pass filter HQ525/50) (Omega Optical), and a water immersion objective (1.2 NA, 60×) (Olympus). Intensity scans were recorded at the plane of the bilayer (X/Y scans) and at a plane perpendicular to it (X/Z scans). The size of X/Y scans was 30×30 μm (400×400 pixels) and that of X/Z scans, 50×20 μm (400×200 pixels). Each pixel was recorded for 1.20 ms.

FCS measurements of lateral diffusion coefficient D of the fluorescently labeled lipid within the bilayer were performed by the *Z*-scan method (described by Benda *et al.* [23]). It has been pointed out that this method is the only artifact-free single focus measurement of lateral diffusion coefficients [24]. It does not require any external calibration and it does not suffer from positioning problems [23]. Numerical simulations have further proved that it is free of the usual artifacts of conventional FCS techniques [24,25]. A set of FCS curves was measured at various Z positions of the focal plane with respect to the bilayer spaced by 0.2 μm. Particular FCS curves were treated according to ref. 23. The average number of particles in the illuminated bilayer surface (PN), and diffusion time (τ_D) show a parabolic dependence on the Z position [23,26]. Then we plotted τ_D *versus* PN/PN_0 (where PN_0 is the particle number when the bilayer is in focus). The dependence is linear according to Humpolickova *et al.* [26] and its linear fit yields the effective diffusion coefficient D_{eff} and the intercept (with τ_D axis) τ_0, which is 0 for free diffusion [26,27]. Average surface concentration c of fluorescent molecules can be calculated from parabolic fit of dependence of PN on Z position.

Bilayers were formed directly in the measurement cell and unbound vesicles were removed by flushing with excess of buffer. Measurements were performed before and after addition of peptide solution and again after one more flushing with excess of buffer.

Ellipsometry

The changes of thickness and surface mass of the layer adsorbed on the solid surface induced by peptides were measured by a null ellipsometer [22,28]. The technique is based on reflection of polarized light (He–Ne laser, Spectra Physics, Mountain View, CA, $\lambda = 632.8$ nm) from reflecting surface and measurement of the two angles Ψ (psi) and Δ (delta) in the expression $\rho = R_p/R_s = \tan\Psi \exp(i\Delta)$, where R_p and R_s are the total reflection coefficients for light polarized parallel and normal to the plane of incidence. Measurements at room temperature were started by determination of Ψ and Δ for the reflecting surface in the cuvette with 3 ml of rapidly stirred buffer. From these readings, the refractive index of surface was determined. To prevent adsorption of vesicles on

DOI: 10.1002/psc

the walls of cuvette the membrane was formed in a separate vessel. Nonbound vesicles were removed by transferring the slide to the ellipsometer cuvette without exposing the slide to the air. After formation of the bilayer new Δ and Ψ were measured every 12–14 s.

After interaction of peptides with membrane the system was flushed with approximately 40 ml of buffer.

Thickness and refractive index of membranes were calculated for an optical three-layer system as described (Benes *et al.* [22] and [28]). The first medium of this system is the buffer mixture with refractive index n_1 (1.33344) and angle of incidence ϕ_1 (68°). The second medium is the buffer-phospholipids-peptide mixture adsorbed on the reflecting surface, with thickness d_2, refractive index n_2, and angle of incidence ϕ_2 (determined by the Snell's law). The third medium is the reflecting surface with (complex) refractive index n_3, and angle of incidence ϕ_3 (determined by the Snell's law).

The surface mass Γ of adsorbed buffer-phopholipids-peptide mixture, expressed in $\mu g/cm^2$, was calculated from the layer thickness d_2 and refractive index n_2, using the relation [28]: $\Gamma = 0.1 \times d_2[L(n_2) - L(n_1)]/[A/M - v \times L(n_1)]$, with the Lorentz factor L defined as $L(n_i) \equiv (n_i^2 - 1)/(n_i^2 + 2)$, where d_2 is expressed in nm; A and M are the molar refractivity and molecular weight of the phospholipids, and v is the specific volume of phospholipids at room temperature. Values of A/M and v in these calculations were 0.274 and 0.89, respectively [28].

RESULTS AND DISCUSSION

Fluorescence intensity scans of the bilayer before and after application of peptide and after flushing with buffer are presented in Figures 1 and 2. For easier comparison all X/Z scans were normalized to the maximum of intensity before peptide addition and all X/Y scans were normalized to the average intensity before peptide addition. Scans of bilayer prior to treatment with peptide indicate that the bilayer was homogenous and confluent. Both peptides caused a decrease in fluorescence intensity and the appearance of inhomogeneities in the lateral distribution of lipids,

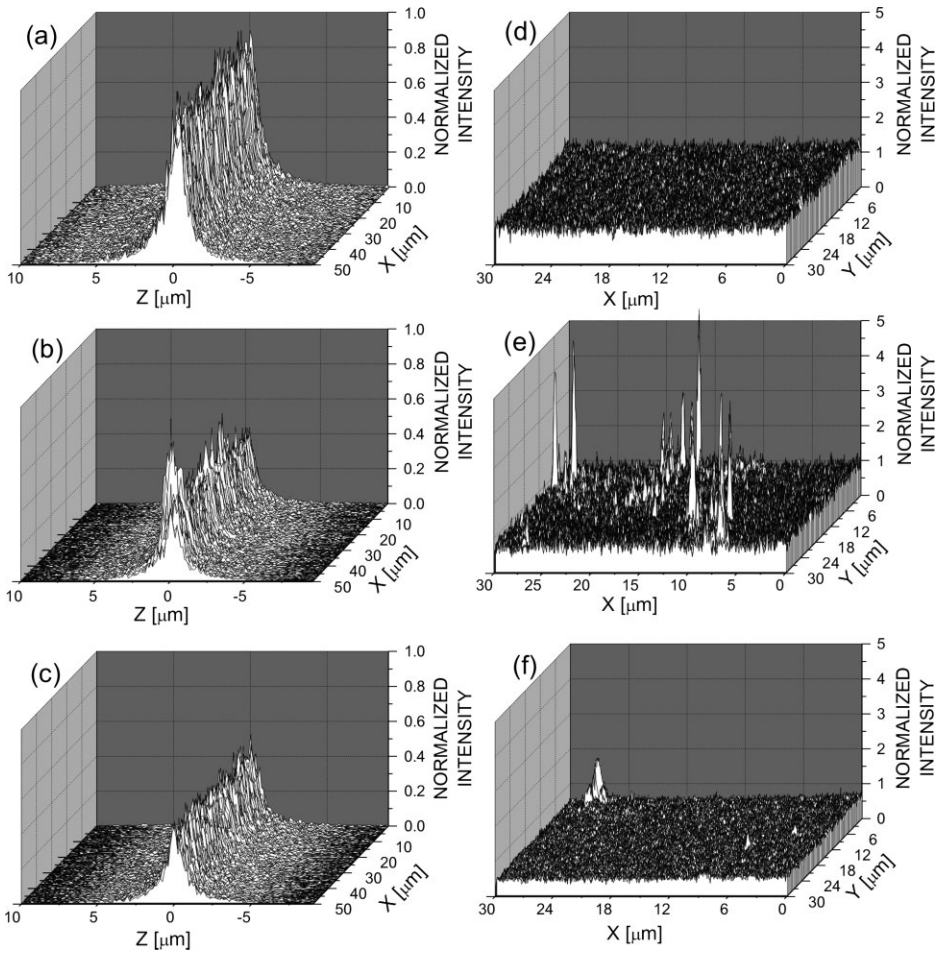

Figure 1 Effect of Crp-4 on fluorescence intensity profiles of SPBs on mica formed of DOPC and DOPS (ratio 4 : 1) and labeled with fluorescence lipid analog Oregon Green 488 DHPE (in the ratio 1 : 10 000) recorded by confocal fluorescence microscope. The size of X/Y scans is 30 × 30 μm (400 × 400 pixels) and that of X/Z scans, 50 × 20 μm (400 × 200 pixels); each pixel was recorded for 1.20 ms. X/Z scans were started 10 μm above the bilayer. X/Z scans were normalized to the maximum of intensity before peptide addition and all X/Y scans were normalized to the average intensity before peptide addition. Figures (a) and (d) show pure SPB; Figures (b) and (e) bilayer after interaction with peptide, and Figures (c) and (f) bilayer after final flushing.

DOI: 10.1002/psc

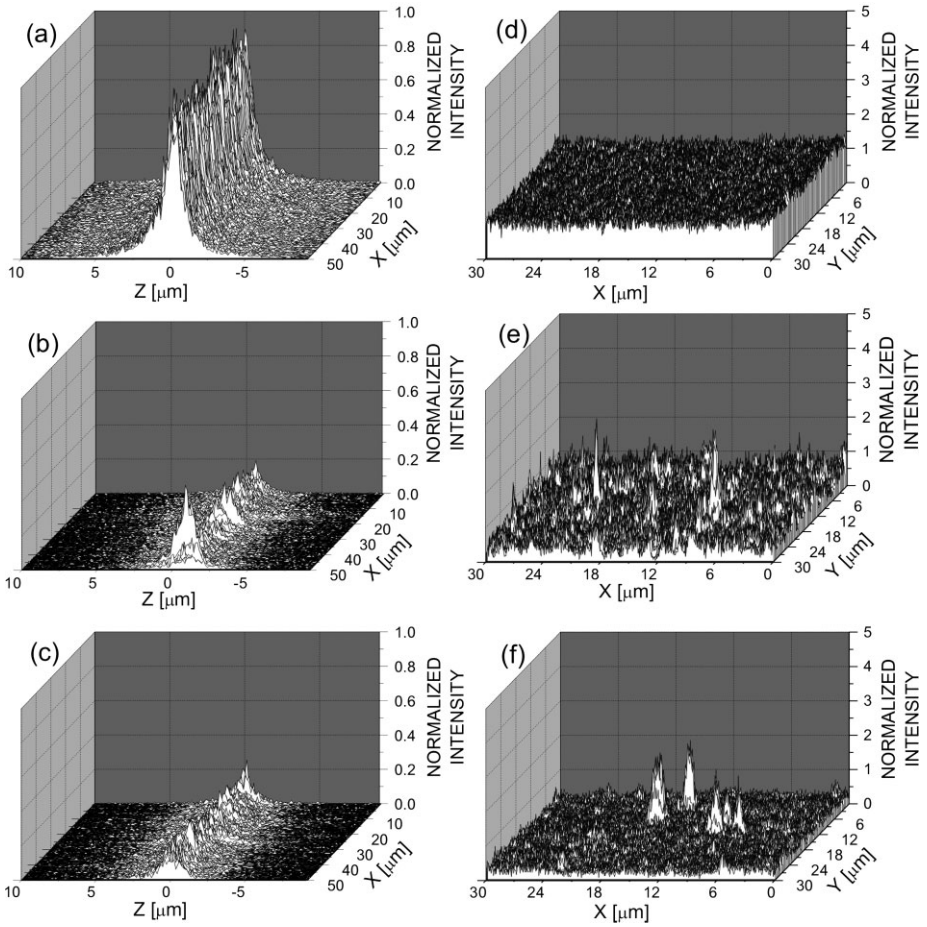

Figure 2 Effect of magainin 2 on fluorescence intensity profiles of SPBs on mica formed of DOPC and DOPS (ratio 4 : 1) and labeled with fluorescence lipid analog Oregon Green 488 DHPE (in the ratio 1 : 10 000) recorded by confocal fluorescence microscope. The size of X/Y scans is 30 × 30 μm (400 × 400 pixels) and that of X/Z scans, 50 × 20 μm (400 × 200 pixels); each pixel was recorded for 1.20 ms. X/Z scans were started 10 μm above the bilayer. X/Z scans were normalized to the maximum of intensity before peptide addition and all X/Y scans were normalized to the average intensity before peptide addition. Figures (a) and (d) show pure SPB; Figures (b) and (e) bilayer after interaction with peptide and Figures (c) and (f) bilayer after final flushing.

but Crp-4 evoked a much smaller decrease in intensity and left the bilayer less perturbed. Flushing of both peptides led to a further decrease in intensity, perhaps due to removal of SPB inhomogeneities.

To estimate the extent of lipid loss induced by treatment with peptides, we calculated the changes of overall fluorescence intensities of the X/Y scans. Some caution is necessary in interpreting these results, because steady-state measurements of bulk fluorescence intensity of a vesicular suspension revealed that interaction with peptide leads by itself to a decrease of intensity to approximately 75% of the original value (data not shown). Since in a bulk experiment in a cuvette no material is lost, this effect can be attributed to peptide-induced fluorescence quenching of the Oregon Green chromophore attached to the lipid. Thus, treatment with Crp-4 in which fluorescence intensity decreased to 72% of the original value (calculated from x/y scan), caused only minor loss of lipids from the bilayer, while lipid loss induced by magainin 2 (37% of original fluorescence intensity) was approximately 50% and significant. Overall, in the case of Crp-4, fluorescence intensities decreased further after flushing to 50%, and in case of magainin 2 to 24% of the original value (prior to peptide application). Moreover, flushing of Crp-4 reduced inhomogeneities in the intensity scans possibly by removing lipid structures loosely bound to the bilayer. The resulting bilayer, however, appeared to be intact after the apparent lipid loss. Flushing does not remove these inhomogeneities completely in the case of magainin 2.

Ellipsometric results also showed differences between Crp-4 and magainin 2–induced effects (Figure 3). For example, the increase in surface mass without altered thickness after application of Crp-4 indicates some peptide insertion which does not change the lipid structure significantly. Flushing with buffer resulted in an immediate decrease in surface mass but still

DOI: 10.1002/psc

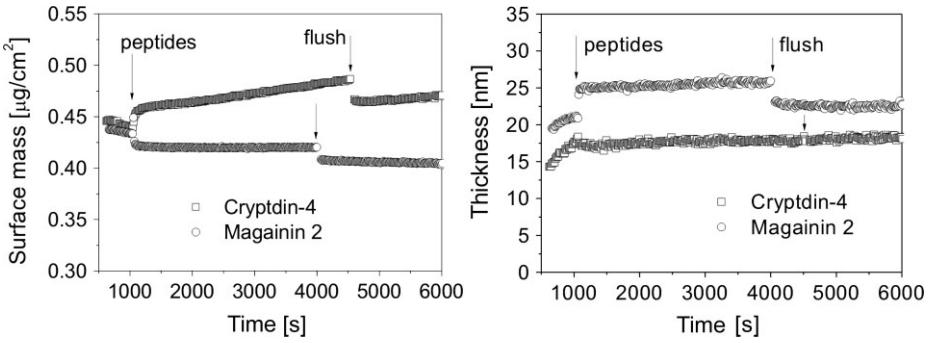

Figure 3 Effect of Crp-4 (□) and magainin 2 (○) on surface mass and thickness of SPBs (formed of DOPC and DOPS in the ratio 4 : 1) adsorbed on silicon slides measured by ellipsometry. Times when peptide solution was added to the sample and when the sample was afterwards flushed with buffer are indicated in the plot.

did not affect thickness. This may be due to removal of certain lipid inhomogeneities as indicated by the results of LSM (Figures 1 and 2) and possibly of some peptide molecules also. Surface mass after flushing is, however, slightly higher than its original value indicating that not all peptide molecules were removed.

Magainin 2 interacts with the membrane differently. A small decrease (approximately 10%) in surface mass suggests that the relatively large loss of lipids deduced from LSM results is partially compensated by peptide adsorption. Further surface mass decrease caused by flushing is likely due to additional lipid and peptide loss. The significant increase in thickness of adsorbed layer after addition of magainin 2 seems to be inconsistent with the results of Ludtke *et al.* [29], whose x-ray diffraction experiments observed SPB thinning induced by magainin 2. This discrepancy can be possibly explained by formation of small lipid structures that protrude from the SPB surface accompanied by thinning of the rest of the bilayer. The formation of fibrillar structures induced by addition of the α-helical AMP temporins and melittin recently were observed by Domanov and Kinnunen [30], and Matsuzaki *et al.*, observed the formation of fibrillar structures induced by magainin 2 [11]. However, the size of these structures depends on the peptide and lipid composition [30]. Inhomogeneities observed in microscopic images can be related to these fibrillar structures but their small size makes evaluation of their parameters (length and thickness) from microscopic images impossible. Flushing with buffer caused decrease in thickness close to its original value, perhaps due to removal of protruding lipid structures, which is consistent with the results of LSM, (Figures 1 and 2) and decrease in surface mass (Figure 3).

Care is needed in comparing the results of ellipsometry and microscopy because the properties of the bilayer may be different in respective cases due to the use of different solid supports (silicon slides are optimal for ellipsometry because the value of their refractive index, but they are not suitable for fluorescence microscopy because of interference effects and fluorescence quenching [22,31]). We have recent evidence that support can influence the way in which AMPs interact with SPBs (data to be published).

Further care is needed because ellipsometric measurements may be subject to systematic errors caused mainly by roughness of reflective surface and nonideal optical components, which can result in overestimation of both thickness d_2 and mass Γ [22]. However, such a source of error would not invalidate observed trends in quantities under study (such as the magainin 2–induced increase in bilayer thickness and the decrease of its mass); only absolute values would be affected. Because conclusions derived from our ellipsometric results are based solely on trends in changes of mass and thickness of adsorbed layer and not on their absolute values, they cannot be influenced by the errors noted above.

Z-scan FCS results for Crp-4 clearly show that the lateral mobility of lipids within the bilayer is reduced by addition of Crp-4, as evident by the decrease in diffusion coefficient (Figure 4 and Table 1). After peptide treatment, the bilayer also is much less homogenous, as shown by larger differences in diffusion properties measured at different points in the SPB and larger differences in surface concentrations of fluorescent lipid analog (Figure 4 and Table 1). Changes induced by peptide are partially reversed by flushing with buffer, perhaps due to only partial removal of peptide molecules from the bilayer, and the SPB again becomes more homogenous in agreement with LSM results. Also, after final flushing, the surface concentration of fluorescent molecules returned to the values prior to peptide addition. The intercept with the diffusion time (τ_D) axis is in all cases close to 0, meaning that the diffusion in the bilayer can be regarded as free and that there are no heterogeneities smaller than the optical resolution of microscope (~250 nm). It was not possible to perform the corresponding experiment with magainin 2, because the bilayer was disintegrated after magainin treatment. It should be pointed out that the LSM experiments, or *Z*-scans at different X/Y positions, and the *Z*-scan at a certain position are complementary in terms

DOI: 10.1002/psc

Table 1 Effect of Crp-4 on parameters of DOPC/DOPS bilayer (ratio 4 : 1) labeled with fluorescent lipid analog Oregon Green 488 DHPE (in the ratio 1 : 100 000) calculated from *Z*-Scan FCS. Values of average surface concentration of fluorescent molecules *c*, effective diffusion coefficient *D* and the intercept of linear fit (with τ_D axis) τ_0 are shown together with their standard errors. See Materials and Methods section for definition of the parameters

	Concentration		Diffusion coefficient		Intercept	
	c (pmol m^{-2})	Δc (pmol m^{-2})	D (μm^2 s^{-1})	ΔD (μm^2 s^{-1})	τ_0 (ms)	$\Delta\tau_o$ (ms)
Pure membrane	30	5	7.5	1.5	−0.2	0.2
With Crp-4	40	10	2.0	0.2	0.7	2.0
After flushing	30	5	4.1	0.6	−0.3	0.3

of their resolution. The size of inhomogeneities observed in the first type of measurements is ~250 nm or larger. *Z*-scan FCS, on the other hand, may provide information on heterogeneities smaller than ~250 nm [26,27].

If Crp-4 and magainin 2 results are compared, it seems that Crp-4 perturbs the bilayer much less. This suggests that the Crp-4 mode of action differs from that of magainin 2. The observed differences in the extent of peptide-induced SPB perturbation are unlikely to be attributable to differences in bactericidal efficiency. Although direct comparisons were not performed here, previous studies suggest that Crp-4 is equally or more bactericidal than magainin 2. For example, Satchell *et al.* [16] found that survival of *E. coli* after exposure to 1 μM Crp-4 was less than 1%, while approximately 10 μM magainin 2 was required for similar effects and 50% of *E. coli* survived after treatment with 1 μM magainin 2 [32]. Therefore, the results indicate a profound difference in the mode of interaction with bilayer of Crp-4 and of α-helical AMPs represented in our study by magainin 2. Satchell *et al.* [9] also observed differences in the mode of action between Crp-4 and melittin, another α-helical peptide. From our experimental results and results presented in previous works [9,10,13,16,17], we conclude that molecules of Crp-4 are inserting transiently and in rapid equilibrium with the bilayer such that only a small fraction of the peptide pool associates with the bilayer at any given time, causing thus only minor perturbation to the bilayer structure.

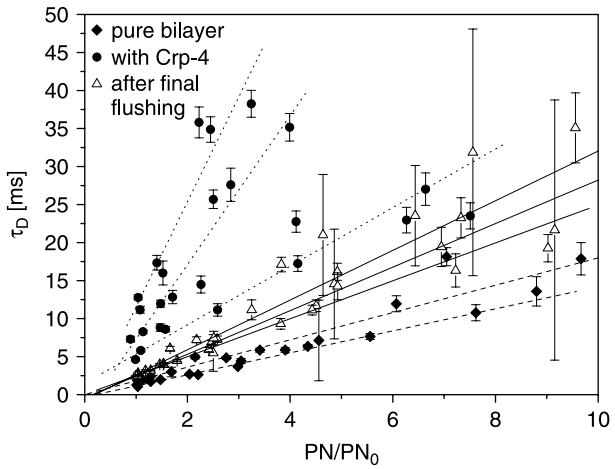

Figure 4 Effect of Crp-4 on mobility of lipids within a bilayer on mica formed of DOPC and DOPS (ratio 4 : 1) and labeled with fluorescent lipid analog Oregon Green 488 DHPE (in the ratio 1 : 100 000) measured by *Z*-scan FCS. The plot shows the diffusion time (τ *D*) *versus* particle number (PN/PN_0) measured at various *Z* positions of the focal plane with respect to the bilayer. Measurements were performed at different points within pure bilayer, bilayer with Crp-4 and bilayer after final flushing and measured points were linearly fitted and fits for individual points are shown in the plot (see Materials and Methods section); higher slopes means slower diffusion. Error bars represent standard errors.

CONCLUSIONS

This study shows that Crp-4, a triple-stranded, β-sheet peptide, interacts with a phospholipid bilayer in a different manner than magainin 2, a prototypical linear AMP that adopts an α-helical structure in membrane mimetic environments. We found that molecules of Crp-4 enter the bilayer without changing its thickness but by making it more rigid. The inserted peptide molecules are not removed completely by flushing the SPB, and the bilayer remains intact. On the other hand, magainin 2 causes a significant apparent increase of thickness of SPBs, and evidence suggests that this results from formation of phospholipid structures that protrude from the bilayer surface. These structures are removable by flushing, leaving the SPB largely damaged. Whether these observed differences in the mechanisms of Crp-4 and magainin 2 interactions with phospholipid bilayer are determined by differences in the secondary structures, distribution of charge and aliphatic side chains, or by the different inherent flexibilities of the respective peptide backbones remains to be determined.

DOI: 10.1002/psc

Acknowledgements

We thank Paavo Kinnunen and Raz Jelinek for discussions. M. H. thanks The National Research Center (LC06063). A.M. thanks the Grant Agency of the Czech Republic via 203/05/H001. A.B. and R.M. thank the Grant Agency of the Czech Republic via 203/05/2308. Also supported by NIH grants AI059346 and DK044632 and by the Human Fronteirs Science Program (A.J.O.).

REFERENCES

1. Zasloff M. Antimicrobial peptides of multicellular organisms. *Nature* 2002; **415**: 389–395.
2. Blondelle SE, Lohner K, Aguilar MI. Lipid-induced conformation and lipid-binding properties of cytolytic and antimicrobial peptides: determination and biological specificity. *Biochim. Biophys. Acta* 1999; **1462**: 89–108.
3. Lehmann J, Retz M, Sidhu SS, Suttmann H, Sell M, Paulsen F, Harder J, Unteregger G, Stockle M. Antitumor activity of the antimicrobial peptide Magainin II against bladder cancer cell lines. *Eur. Urol.* 2006; **50**: 141–147.
4. Cruciani R, Barker J, Zasloff M, Chen H, Colamonici O. Antibiotic magainins exert cytolytic activity against transformed-cell lines through channel formation. *Proc. Natl. Acad. Sci. U.S.A.* 1991; **88**: 3792–3796.
5. Bechinger B. The structure, dynamics and orientation of antimicrobial peptides in membranes by multidimensional solid-state NMR spectroscopy. *Biochim. Biophys. Acta* 1999; **1462**: 157–183.
6. Shai Y. Mechanism of the binding, insertion and destabilization of phospholipid bilayer membranes by α-helical antimicrobial and cell non-selective membrane-lytic peptides. *Biochim. Biophys. Acta* 1999; **1462**: 55–70.
7. Ramamoorthy A, Thennarasu S, Lee DK, Tan A, Maloy L. Solid-state NMR investigation of the membrane-disrupting mechanism of antimicrobial peptides MSI-78 and MSI-594 derived from magainin 2 and melittin. *Biophys. J.* 2006; **91**: 206–216.
8. Ouellette AJ, Selsted ME. Paneth cell defensins: Endogenous peptide components of intestinal host defense. *FASEB J.* 1996; **10**: 1280–1289.
9. Satchell DP, Sheynis T, Shirafuji Y, Kolusheva S, Ouellette AJ, Jelinek R. Interactions of mouse paneth cell alpha-defensins and alpha-defensin precursors with membranes. *J. Biol. Chem.* 2003; **278**: 13838–13846.
10. Tanabe H, Qu XQ, Weeks CS. Structure-activity determinants in Paneth cell alpha-defensins – Loss-of-function in mouse cryptdin-4 by charge-reversal at arginine residue positions. *J. Biol. Chem.* 2004; **279**: 11976–11983.
11. Matsuzaki K, Sugishita K, Harada M, Fujii N, Miyajima K. Interactions of an antimicrobial peptide, magainin 2, with outer and inner membranes of Gram-negative bacteria. *Biochim. Biophys. Acta* 1997; **1327**: 119–130.
12. Papo N, Shai Y. Exploring peptide membrane interaction using surface plasmon resonance: Differentiation between pore formation versus membrane disruption by lytic peptides. *Biochemistry* 2003; **42**: 458–466.
13. Sheynis T, Sykora J, Benda A, Kolusheva S, Hof M, Jelinek R. Bilayer localization of membrane-active peptides studied in biomimetic vesicles by visible and fluorescence spectroscopies. *Eur. J. Biochem.* 2003; **270**: 4478–4487.
14. Dathe M, Wieprecht T. Structural features of helical antimicrobial peptides: their potential to modulate activity on model membranes and biological cells. *Biochim. Biophys. Acta* 1999; **1462**: 71–87.
15. Tamba Y, Yamazaki M. Single giant unilamellar vesicle method reveals effect of antimicrobial peptide magainin 2 on membrane permeability. *Biochemistry* 2005; **44**: 15823–15833.
16. Satchell DP, Sheynis T, Kolusheva S, Cummings J, Vanderlick TK, Jelinek R, Selsted ME, Ouellette AJ. Quantitative interactions between cryptdin-4 amino terminal variants and membranes. *Peptides* 2003; **24**: 1795–1805.
17. Weeks CS, Tanabe H, Cummings JE, Crampton SP, Sheynis T, Jelinek R, Vanderlick TK, Cocco MJ, Ouellette AJ. Matrix metalloproteinase-7 activation of mouse Paneth cell pro-alpha-defensins – SER43 down arrow ILE44 proteolysis enables membrane-disruptive activity. *J. Biol. Chem.* 2006; **281**: 28932–28942.
18. Shirafuji Y, Tanabe H, Satchell DP, Henschen-Edman A, Wilson CL, Ouellette AJ. Structural determinants of procryptdin recognition and cleavage by matrix metalloproteinase-7. *J. Biol. Chem.* 2003; **278**: 7910–7919.
19. Wilson CL, Ouellette AJ, Satchell DP, Ayabe T, Lopez-Boado YS, Stratman JL, Hultgren SJ, Matrisian LM, Parks WC. Regulation of intestinal alpha-defensin activation by the metalloproteinase matrilysin in innate host defense. *Science* 1999; **286**: 113–117.
20. White SH, Wimley WC, Selsted ME. Structure, function, and membrane integration of defensins. *Curr. Opin. Biotechnol.* 1995; **5**: 521–527.
21. Selsted ME. Investigational approaches for studying the structures and biological functions of myeloid antimicrobial peptides. In *Genetic Engineering: Principles and Methods*, Setlow JK (ed.). Plenum Press: New York, 1993; 131–147.
22. Benes M, Billy D, Benda A, Speijer H, Hof M, Hermens WT. Surface-dependent transitions during self-assembly of phospholipid membranes on mica, silica and glass. *Langmuir* 2004; **20**: 10129–10137.
23. Benda A, Benes M, Marecek V, Lhotsky A, Hermens WT, Hof M. How to determine diffusion coefficients in planar phospholipid systems by confocal fluorescence correlation spectroscopy. *Langmuir* 2003; **19**: 4120–4126.
24. Dertinger T, Pacheco V, von der Hocht I, Hartmann R, Gregor I, Enderlein J. Two-focus fluorescence correlation spectroscopy: A new tool for the accurate and absolute diffusion measurements. *Eur. J. chem. phy. chem.* 2007; **8**: 433–443.
25. Enderlein J, Gregor I, Patra D, Fitter J. Art and artefacts of fluorescence correlation spectroscopy. *Curr. Pharm. Biotechnol.* 2004; **5**: 155–161.
26. Humpolickova J, Gielen E, Benda A, Fagulova V, Vercammen J, Vandeven M, Hof M, Ameloot M, Engelborghs Y. Probing diffusion laws within cellular membranes by Z-scan fluorescence correlation spectroscopy. *Biophys. J.* 2006; **91**: L23–L25.
27. Wawrezinieck L, Rigneault H, Marguet D, Lenne PF. Fluorescence correlation spectroscopy diffusion laws to probe the submicron cell membrane organization. *Biophys. J.* 2005; **89**: 4029–4042.
28. Cuypers PA, Corsel JW, Janssen MP, Kop JMM, Hermens WT, Hemker HC. The adsorption of prothrombin to phosphatidylserine multilayers quantitated by ellipsometry. *J. Biol. Chem.* 1983; **258**: 2426–2431.
29. Ludtke S, He K, Huang H. Membrane thinning caused by magainin 2. *Biochemistry* 1995; **34**: 16764–16769.
30. Domanov YA, Kinnunen PKJ. Antimicrobial peptides temporins B and L induce formation of tubular lipid protrusions from supported phospholipid bilayers. *Biophys. J.* 2006; **91**: 4427–4439.
31. Benda A, Fagulova V, Deyneka A, Enderlein J, Hof M. Fluorescence lifetime correlation spectroscopy combined with lifetime tuning: New perspectives in supported phospholipid bilayer research. *Langmuir* 2006; **22**: 9580–9585.
32. Bucki R, Pastore JJ, Randhawa P, Vegners R, Weiner DJ, Janmey PA. Antibacterial activities of rhodamine B-conjugated gelsolin-derived peptides compared to those of the antimicrobial peptides cathelicidin LL37, magainin II and melittin. *Antimicrob. Agents Chemother.* 2004; **48**: 1526–1533.